



저작자표시-비영리-변경금지 2.0 대한민국

이용자는 아래의 조건을 따르는 경우에 한하여 자유롭게

- 이 저작물을 복제, 배포, 전송, 전시, 공연 및 방송할 수 있습니다.

다음과 같은 조건을 따라야 합니다:



저작자표시. 귀하는 원저작자를 표시하여야 합니다.



비영리. 귀하는 이 저작물을 영리 목적으로 이용할 수 없습니다.



변경금지. 귀하는 이 저작물을 개작, 변형 또는 가공할 수 없습니다.

- 귀하는, 이 저작물의 재이용이나 배포의 경우, 이 저작물에 적용된 이용허락조건을 명확하게 나타내어야 합니다.
- 저작권자로부터 별도의 허가를 받으면 이러한 조건들은 적용되지 않습니다.

저작권법에 따른 이용자의 권리는 위의 내용에 의하여 영향을 받지 않습니다.

이것은 [이용허락규약\(Legal Code\)](#)을 이해하기 쉽게 요약한 것입니다.

[Disclaimer](#)

A Doctoral Dissertation

Evaluation of the Cuttlebone as a Bone Graft Substitute

Department of Veterinary Medicine
GRADUATE SCHOOL
JEJU NATIONAL UNIVERSITY

Sangcheol Won

June, 2011

Evaluation of the Cuttlebone
as a Bone Graft Substitute

Sangcheol Won

(Supervised by professor Jongtae Cheong)

A thesis submitted in partial fulfillment of the requirement for the
degree of Doctor of Philosophy in Veterinary Medicine

2011. 06.

This thesis has been examined and approved.

.....
Thesis director, Kyoung-Kap Lee, Prof. of Dept. of Veterinary Medicine

.....
Jongtae Cheong, Prof. of Dept. of Veterinary Medicine

.....
Nam-Soo Kim, Prof. of Dept. of Veterinary Medicine

.....
Jae-Hoon Kim, Prof. of Dept. of Veterinary Medicine

.....
Joo-Myoung Lee, Prof. of Dept. of Veterinary Medicine

.....
Date

Department of Veterinary Medicine
GRADUATE SCHOOL
JEJU NATIONAL UNIVERSITY

CONTENTS

ABSTRACT	1
LIST OF ABBREVIATIONS	3
LIST OF TABLES	4
LIST OF FIGURES	5
GENERAL INTRODUCTION	7

CHAPTER I.


Evaluation of the Biocompatibility of Cuttlebone in Mouse

I-1 INTRODUCTION	11
I-2 MATERIALS AND METHODS	13
I-3 RESULTS	18
I-4 DISCUSSION	22

CHAPTER II.

Evaluation of the Bone Defect Regeneration after Implantation with Cuttlebone in Rabbit

II-1 INTRODUCTION	26
II-2 MATERIALS AND METHODS	29



The logo of Jeju National University is a large, stylized 'J' shape. The left vertical stroke of the 'J' is composed of three curved, flame-like shapes in blue, green, and grey. The bottom horizontal stroke is a solid purple bar. In the center of the 'J', there is a small icon of an open book with a star above it, and the text 'JEJU 1952' below it. The entire logo is set against a background of a large, faint watermark of the university's name in English and Korean.

II-3 RESULTS	35
II-4 DISCUSSION	43
CONCLUSIONS	47
REFERENCES	48
ABSTRACT IN KOREAN	63

Evaluation of the Cuttlebone as a Bone Graft Substitute

Sangcheol Won

(Supervised by professor Jongtae Cheong)

Department of Veterinary Medicine
Graduate School, Jeju National University
Jeju, Korea

Abstract

Bone grafting is widely used to bridge major bone defects or to promote bone union. Natural calcium carbonate has been used as a bone substitute material and used to scaffold for bone morphogenetic protein (BMP). The aims of this study were to evaluate the biocompatibility of cuttlebone (CB) and hydroxyapatite (HA) from CB (CBHA), and to evaluate the bone defect regeneration of CB, CBHA, and HA from coral (CHA). Each material was shaped into disks (5 mm in diameter and 2 mm in thickness). To test biocompatibility, the disks were implanted into the dorsal subcutaneous tissue in mice. Fibrous capsule thickness around each disk was evaluated histologically at 2 and 4 weeks after implantation. In the evaluation of bone defect regeneration, 5 mm-diameter defects were created in rabbit calvaria. Concerning biocompatibility, fibrous capsule thickness of CBHA was significantly thinner than that of CB and CHA ($p < 0.05$) at 2 and 4 weeks

after implantation. Concerning 12-week total changes of radiologic Gray-level histogram, CBHA was significantly higher than CHA ($p<0.05$). In the evaluation of bone defect regeneration, bone formation of CHA was significantly higher than that of CB and CBHA ($p<0.05$). Based on the clinical and histological results, CBHA would be a safe material for use inside the body and has more effective osteoconduction than CB. It is suggested that CBHA is a valuable bone graft material.

Key words; Bone Graft, Calcium Carbonate, Cuttlebone, Hydroxyapatite, Scaffold

List of Abbreviations

BMP	Bone morphogenetic protein
CB	Cuttlebone
CB1	Cuttlebone after defatting and freeze-drying
CB1bmp	CB1 with rhBMP-2
CB2	Cuttlebone after removing organic components
CBHA	Hydroxyapatite from cuttlebone 2
CC	Calcium carbonate
CHA	Hydroxyapatite from coral
FGF	Fibroblast growth factor
HA	Hydroxyapatite
IGF	Insulin-like growth factor
PDGF	Platelet derived growth factor
rhBMP-2	Recombinant human bone morphogenetic protein 2
TGF- β	Transforming growth factor-beta

List of Tables

Table 1. Experimental design for the assessment of biocompatibility of the implants in mice ----- 16

Table 2. Experimental design for the bone defect regeneration in rabbits ----- 30

List of Figures

- Fig 1. Preparation of CB1 for implantation ----- 14
- Fig 2. Preparation of CB2 for implantation ----- 14
- Fig 3. CB1, CB2, CBHA, and CHA implants were shaped cylindrical disks about 5 mm in diameter and 2 mm in thickness----- 15
- Fig 4. Schematic drawing for applied implants in subcutaneous tissue in mice (a) and photograph of applied implants (b) ----- 16
- Fig 5. X-ray diffraction patterns of HA (JCPDS # 09-0432) (a) and products prepared by hydrothermal reaction of CB2 (b) ----- 18
- Fig 6. Thickness of fibrous capsule surrounding CB1, CB2, CBHA, and CHA implants measured at 2 and 4 weeks after implantation in mice ----- 20
- Fig 7. Granulation tissue formation (arrowheads) around graft materials (G) in group CB2 (a) and CBHA (b) at 2 weeks after implantation ----- 21
- Fig 8. Granulation tissue formation (arrowheads) around graft materials (G) in group CB2 (a) and CBHA (b) at 4 weeks after implantation ----- 21
- Fig 9. Photographs of rabbit calvarial defect (\varnothing 5 mm) formation (a) and calvarial defects filled with CB1, CB1bmp, and CHA (b) ----- 31

Fig 10. Photographs of rabbit calvarial defect formation (a) and calvarial defects filled with CB2 and CBHA (b) ----- 31

Fig 11. Histogram processing of radiograph by Photoshop program ----- 33

Fig 12. Measurement of bone defect regeneration in rabbit calvaria by histomorphometric parameters ----- 34

Fig 13. Total 12-week changes of Gray-level histogram in each specimen ----- 37

Fig 14. The rate of bone defect regeneration group CB1, CB2, CB1bmp, CBHA, and CHA specimens ----- 38

Fig 15. Histologic sections of group CB1 (a), CB1bmp (b), CB2 (c), CBHA (d), and CHA (e) at 4 weeks after implantation ----- 40

Fig 16. Histologic sections of group CB1 (a), CB1bmp (b), CB2 (c), CBHA (d), and CHA (e) at 12 weeks after implantation ----- 41

Fig 17. Histologic features of new bone formation in group CB1 (a), CB1bmp (b), CB2 (c), and CBHA (d) at 12 weeks after implantation ----- 42

GENERAL INTRODUCTION

A bone graft may be the critical factor between successful bone union and catastrophic failure (Millis and Martinez, 2002). Bone grafting is widely-used to bridge major defects or to establish the continuity of the long bone, to aid in fusion of joints, to fill cavities or defects, and to promote bone union in delayed union and nonunion fractures (Finkemeier, 2002; Millis and Martinez, 2002; Piermattei and Flo, 1997). Depending on the type of bone graft, a particular graft may provide a source of live bone cells or osteoinductive factors, give mechanical stability, or act as a scaffold for new bone growth (Millis and Martinez, 2002; Piermattei and Flo, 1997).

Bone grafts or bone graft substitutes are named according to their origin and composition (Johnson and Hulse, 2002; Millis and Martinez, 2002). Autograft bone is transplanted from one site to another in the same animal (Johnson and Hulse, 2002). The current gold standard for bone grafts is the autogenous bone graft (Carson and Bostrom, 2007). Such grafts are histocompatible with host immune systems and will not initiate rejection responses (Millis and Martinez, 2002; Stevenson, 1987). Allograft bone is transplanted from one animal to another of the same species (Johnson and Hulse, 2002). Cellular antigens of these grafts may be recognized as foreign body by the host's immune systems, resulting in graft rejection (Millis and Martinez, 2002; Stevenson, 1987). Xenograft bone is transplanted from one animal to another of a different species (Johnson and Hulse, 2002). It presents similar problem to the allograft (Kim, 2008; Millis and Martinez, 2002).

Bone graft substitutes contain many types of materials, including biomaterials, ceramics, and calcium ceramics. Biomaterials consist of metals (Kim, 1998), polymers (Kim *et al.*, 2008a), and ceramics: bioactive glass (Froum *et al.*, 1998; Macedo *et al.*, 2004; Ryu *et al.*, 2000). Calcium ceramics

consist of calcium sulfate (Walsh *et al.*, 2003), calcium phosphate (Lee *et al.*, 2007b; LeGeros, 2002; Tadic and Epple, 2004), and calcium carbonate (CC; CaCO_3) (Lee *et al.*, 2008a; Vuola *et al.*, 2000). In ceramic biomaterials, bioabsorbable, and bioactive substances are able to physically bond directly to the host bed, whereas bioinert substances never actually bond to the bone (Carson and Bostrom, 2007).

The composition of bone grafts may include cancellous bone, cortical bone, corticocancellous bone, bone marrow, or bone and articular cartilage: osteochondral (Millis and Martinez, 2002). Cancellous bone grafts consist of highly cellular trabecular bone removed from the medullary cavity of long bone metaphyseal regions (Millis and Martinez, 2002). Their primary advantage is to stimulate and produce new bone (Millis and Martinez, 2002). Cortical bone grafts consist of the dense outer cortical bone that provides structural support (Millis and Martinez, 2002). Corticocancellous grafts are a combination of both cortical and cancellous bone (Millis and Martinez, 2002). Bone marrow is used to provide live undifferentiated mesenchymal cells (Millis and Martinez, 2002). A composite graft is one in which cancellous bone or bone marrow is added to a preserved cortical allograft (Millis and Martinez, 2002). An osteochondral bone graft consists of articular cartilage and associated subchondral bone; the intended use of this graft is to resurface joints, but successful long-term application remains a problem and it is not commonly used (Millis and Martinez, 2002).

The ideal scaffold should provide an initial support for osteoprogenitor cells to deposit mineralized bone matrix; it should be slowly resorbed at the same time the newly formed bone tissue grows inside the scaffold (Mastrogiacomo *et al.*, 2005). A high porosity and a high degree of interconnection among the pores are absolute requirements for the vascularization of the implant and for new bone formation (Mastrogiacomo *et al.*, 2005). In addition, ideal bone graft substitutes should provide four elements: an osteoconductive matrix, which is

a nonviable scaffolding conducive to bone ingrowth; osteoinductive factors, which are the chemical agents that induce the various stages of bone regeneration and repair; osteogenic cells, which have the potential to differentiate and facilitate the various stages of bone regeneration; and structural integrity (Gazdag *et al.*, 1995; Ilan and Ladd, 2003).

Natural CC such as coral (Guillemin *et al.*, 1987; Vuola *et al.*, 1996, 1998, 2000), eggshell (Dupoirieux *et al.*, 1995, 1999, 2001a; Durmuş *et al.*, 2007; Lee *et al.*, 2008a) has been used as a bone substitute material. Through a hydrothermal reaction, the CaCO_3 skeleton of CC is changed to hydroxyapatite (HA: $\text{Ca}_{10}(\text{PO}_4)_6(\text{OH})_2$). HA has been isolated from coral (CHA) (Chou *et al.*, 2007; Holmes *et al.*, 1984; LeGeros, 2002; Roy and Linnehan, 1974; Sivakumar *et al.*, 1996; Xu *et al.*, 2001), eggshell (Park *et al.*, 2008; Park *et al.*, 2009), and cuttlebone (CBHA) (Ivankovic *et al.*, 2009, 2010; Kim *et al.*, 2008b; Wang *et al.*, 2001; Xing *et al.*, 2007). The basic difference between HA and CC is that CC is biodegradable and HA is not or only very little (Vuola *et al.*, 1996). Porous HA is biocompatible and osteoinductive (Chiroff *et al.*, 1975). HA has attracted a great deal of interest as a biomaterial for implants and bone augmentation since its chemical composition is close to that of bone (Kim *et al.*, 2008b). Cuttlebone (CB), which is composed of CC has a porous structure with all pore interconnected throughout the skeleton and CB.

The purpose of this study was to evaluate the biocompatibility of CB in mouse model and to evaluate the bone defect regeneration of CB in a rabbit calvarial defect model.

CHAPTER I

Evaluation of the Biocompatibility of Cuttlebone in Mouse

I -1. Introduction

The development of new biomedical devices from various materials has received a great deal of attention recently (Butler *et al.*, 2001). When a material is intended for safe use inside the body, its *in vivo* performance and biocompatibility must be scrupulously verified (Ryhänen *et al.*, 1998).

Measuring the thickness of an encapsulating membrane around the implant is a basic tool for estimating biocompatibility (Ryhänen *et al.*, 1998). Utilization of the thickness of the scar capsule around an implant alone is problematic because there are factors other than the material itself that can affect capsular thickness (Ryhänen *et al.*, 1998). The fibrous tissue includes inflammatory components such as macrophages, fibroblasts, neutrophils, collagen, and numerous blood vessels (Butler *et al.*, 2001), and capsule formation depends on various factors, including implant size (Aalto and Heppleston, 1984), shape (Matlaga *et al.*, 1976), surface texture (Behling and Spector, 1986), surface chemistry (Clark *et al.*, 1976), pore size (White *et al.*, 1981), and implantation site (Bakker *et al.*, 1988). Subcutaneous implantation of biomaterials induces acute and chronic inflammatory reactions resulting in fibrous tissue formation around the device (Butler *et al.*, 2001). Thickness appears to directly correspond with the other cellular components present in the fibrous tissue matrix (Butler *et al.*, 2001). The tissue and cellular responses to implants are screened on the basis of morphologic observations on routine histologic evaluation (Butler *et al.*, 2001).

Commonly, biocompatibility of bone graft substitutes and scaffolds are investigated by two types of *in vivo* tests: subcutaneous implant in mice (Kim *et al.*, 2004; Lee *et al.*, 2006; Yeom *et al.*, 2007) or rats (Butler *et al.*, 2001; Lehle *et al.*, 2004; Li *et al.*, 1999), and calvarial defect models

employing rabbits (Durmuş *et al.*, 2007; Gu *et al.*, 2009; Kim *et al.*, 2008a) or rats (Bosch *et al.*, 1995; Dupoirieux *et al.*, 2001b; Lee *et al.*, 2008a, 2008b; Park *et al.*, 2008). Typically, before the implant, biomaterials are prepared to eliminate the immune response.

The purpose of this study was to compare tissue responses after implantation of CB in a mouse model. Furthermore, the thickness of fibrous capsule surrounding specimens was measured by histologic analysis.

I -2. Materials and Methods

I -2-1. Fabrication of implants

Three kinds of implants (CB1, CB2 and CBHA) were prepared from the same genus of cuttle bone (*Sepia esculenta*). The CHA implants used consisted of HA from coral (BoneMedik[®], Metabiomed, Korea). The CB1 implants were processed in several steps that included defatting, freezing, drying, and sterilization (Fig 1, Choi *et al.*, 2003; Choi and Lee, 1998). The CB2 implants were processed by removing organic components, washing, drying, and sterilizing (Fig 2, Kim *et al.*, 2008b).

CBHA implants were processed in hydrothermal synthesis: CB2 was put in 2M(NH₄)₂HPO₄ in a Teflon[®] lined hydrothermal bomb (Hydrothermal Reactor System[®], Hanwoul Engineering, Korea) and heated for 16 h at 180°C. Then, the block was immersed in 2M (NH₄)₂HPO₄ and treated at 200°C for 24 h hydrothermally. After thoroughly washing with distilled water, the block was dried at 90°C (Kim *et al.*, 2008b). After X-ray diffraction (XRD) examination of the block, it was used as CBHA. These implants were shaped into cylindrical disks about 5 mm in diameter and 2 mm in thickness (Fig 3) and were sterilized by ethylene oxide gas.

I -2-2. Experimental animals and surgical procedure

Twenty 9-week-old, 22 ± 0.2 g male BALB/c mice were used in the experiments. They were housed under a standard light-dark schedule, were fed a stock diet and had access to tap water *ad libitum*.

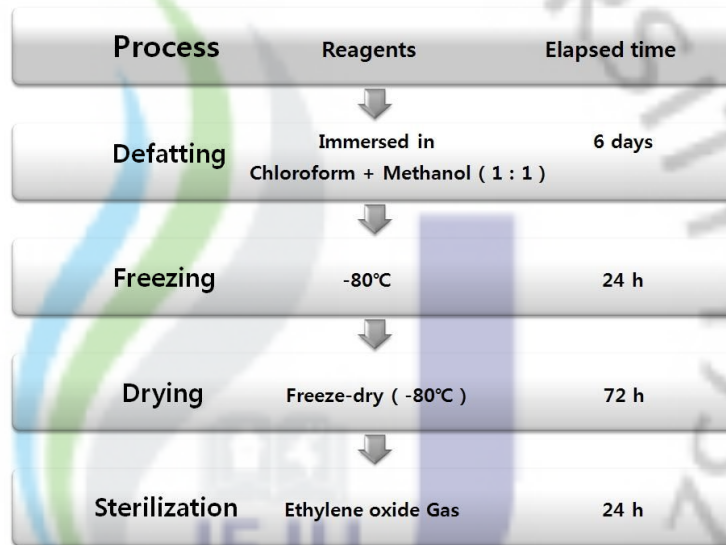


Fig 1. Preparation of CB1 for implantation. The CB1 implants were processed through defatting, freezing, drying, and sterilization.

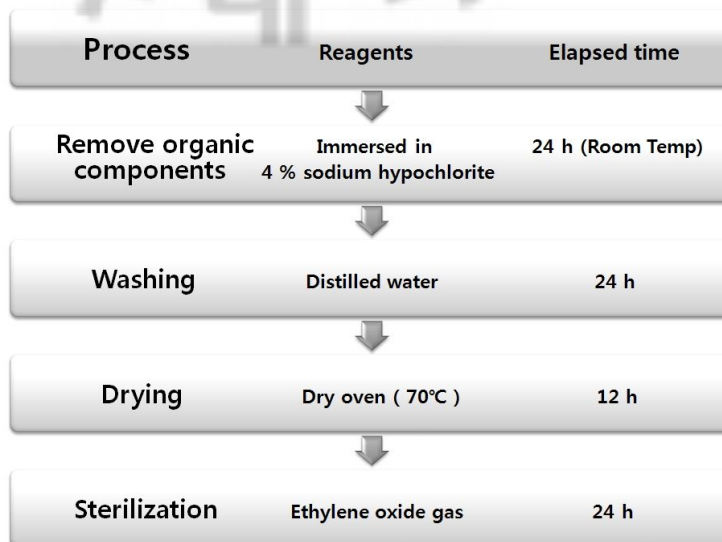


Fig 2. Preparation of CB2 for implantation. The CB2 implants were processed through removing organic components, washing, drying, and sterilization.



Fig 3. CB1, CB2, CBHA, and CHA implants were shaped cylindrical disks about 5 mm in diameter and 2 mm in thickness and were sterilized by ethylene oxide gas.

The experimental protocol was approved by the Animal Care and Use Committee, Jeju National University (approval number 2010-0042). The mice were divided into four experimental groups as shown in Table 1. Aseptic surgical technique was applied during the surgical procedure. Mice were anesthetized by the intramuscular injection of a dose of tiletamine/zolazepam (Zoletil50[®], Virbac, France). After the anesthesia, the middle of the back of each mouse was shaved. The incision sites were washed with 70% ethanol and scrubbed with 10% povidone iodine, and a skin incision with 1.5 cm in length was made. Sterilized implants were inserted subcutaneously through the incision site (Fig 4) and the wound was closed with 4-0 nylon. Immediately following implantation, the mice were injected subcutaneously with a dose of gentamicin sulfate (Gentamicin 5% Inj.[®], Daesung Microbiological Labs., Korea) for 3 days.

Table 1. Experimental design for the assessment of biocompatibility of the implants in mice

Mice	Group	Application	
		Site	Type of implants
n = 10	CB1	L. Dorsal back SQ	Cuttlebone 1
	CHA	R. Dorsal back SQ	HA from coral
n = 10	CB2	L. Dorsal back SQ	Cuttlebone 2
	CBHA	R. Dorsal back SQ	HA from cuttlebone

L.: Left, R.: Right, n: number of experimental animal, CB: Cuttlebone, HA: Hydroxyapatite, SQ: Subcutis

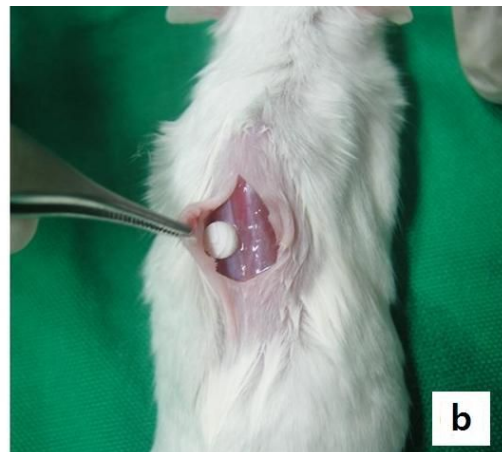
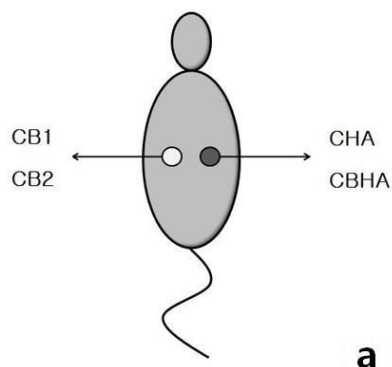


Fig 4. Schematic drawing for applied implants in subcutaneous tissue in mice (a). Photograph of applied implants (b). Sterilized implants were inserted subcutaneously through the incision site.

I-2-3. Histologic investigations and analysis of fibrous capsular membrane thickness

Ten mice were euthanized at 2 and 4 weeks after surgery. Implanted disks and the surrounding tissue were removed as a single mass and immediately immersed in 10% phosphate-buffered formalin for 3 days. The mass was decalcified for at least 7 days using 5% formic acid. Implants were dehydrated in an ethanol series, embedded in paraffin, and cut into 6 mm-thick sections. The sections were stained with hematoxylin and eosin (H&E) stain and Masson's trichrome stain. The fibrous capsular membrane thickness around the implants was determined with a CCD camera-based digital image analysis system. The system consisted of a microscope (Olympus BX41; Japan) and an Olympus DP20 video camera. The fibrous capsular membrane thickness was determined at each point of the horizontal and vertical lines. The fibrous capsular membrane thickness was expressed as a mean value of eight hits.

I-2-4. Statistical analysis

The Statistical Package for the Social Science version 17.0 software (SPSS, USA) was used for data analysis. Mann-Whitney's u -test was used to evaluate differences between each group. A p value ≤ 0.05 was considered statistically significant.

I -3. Results

I -3-1. Characterization CBHA

The typical X-ray diffraction (XRD) patterns of product prepared by hydrothermal reaction of CB2 at 200°C for 24 h are shown in Fig 5. The XRD patterns of the CB were confirmed as HA on the basis of JCPDS card #09-0432. They were completely transformed into HA by hydrothermal reaction.

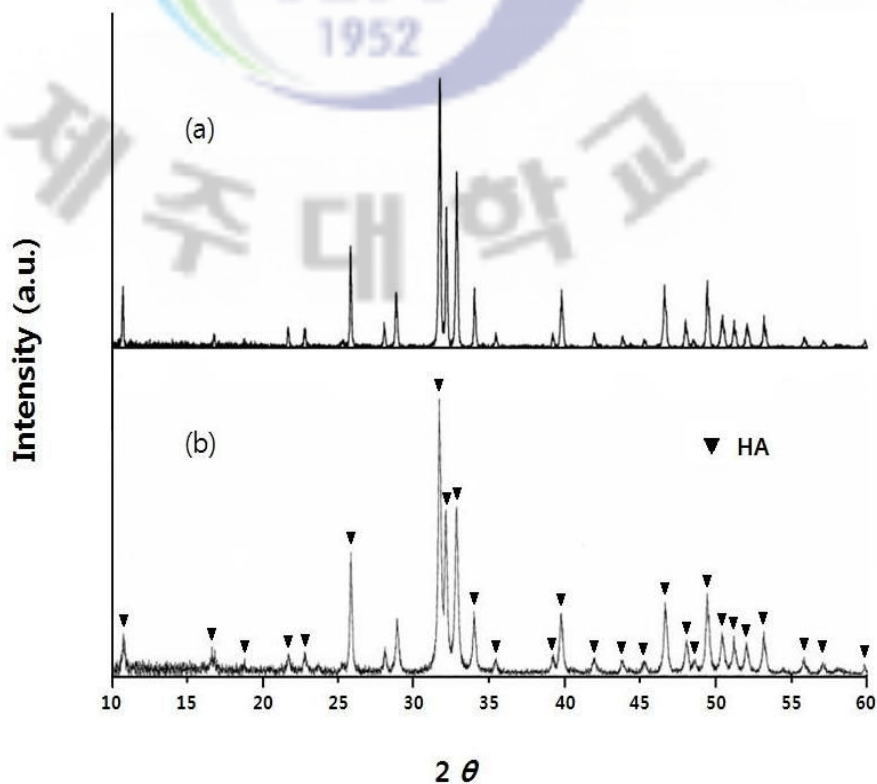


Fig 5. X-ray diffraction patterns of HA (JCPDS # 09-0432) (a) and products prepared by hydrothermal reaction of CB2 (b). Arrows indicate the picks of HA.

I-3-2. Analysis of fibrous capsular membrane thickness

The analytical results of fibrous capsular membrane thickness are shown in Fig 6. At 2 weeks, the thickness of fibrous capsule in group CBHA was significantly lower than that of other groups. Groups CB1, CB2, and CHA displayed no significant differences. At 4 weeks, the thickness of the fibrous capsule in group CB1 was significantly higher than that of other groups. In group CBHA, the thickness of the fibrous capsule was significantly lower than that of other groups. There was no significant difference between group CB2 and CHA. In all groups, the thickness of fibrous capsules at 4 weeks was thinner than at 2 weeks.

I-3-3. Histologic evaluation

At 2 weeks after implantation, all graft materials in the subcutis were surrounded by mild to moderate dense fibrous stroma composed of abundant collagenous fiber than stained blue upon Masson's trichrome staining (Fig 7). Variable numbers of inflammatory cells such as neutrophils, macrophages, and foreign body giant cells had infiltrated around the graft materials. Some blood vessels in the subcutis showed marked congestion. At 4 weeks after implantation, fibrous stromal reaction and inflammatory reaction around graft materials had gradually decreased compared to the mice observed 2 weeks (Fig 8). Occasionally, new formed capillaries were observed in the proliferated fibrous stroma.

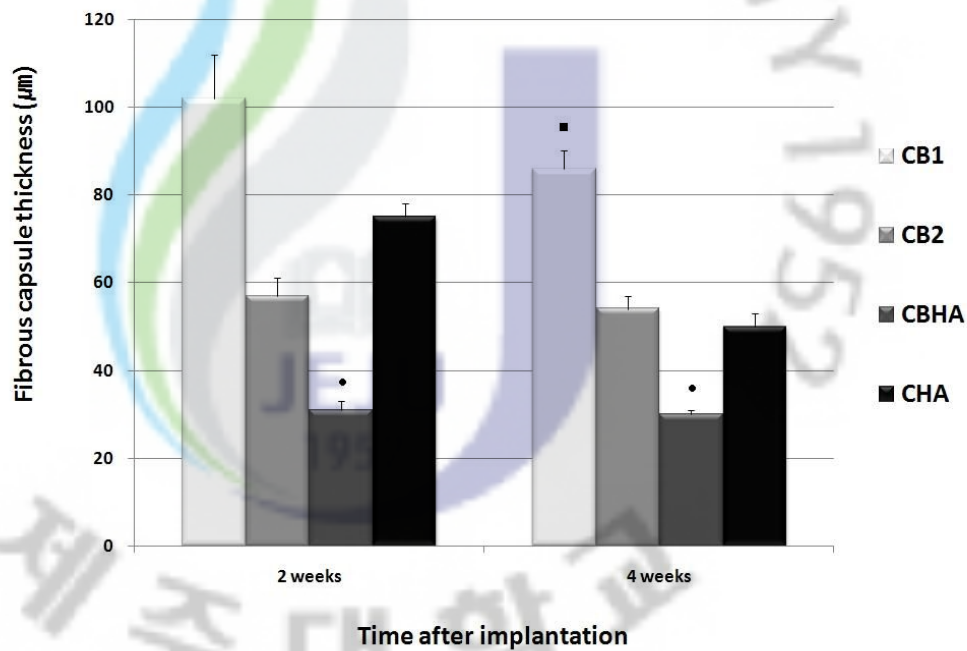


Fig 6. Thickness of fibrous capsule surrounding CB1, CB2, CBHA, and CHA implants measured at 2 and 4 weeks after implantation in mice. Values are expressed as mean \pm SE.

- Significantly lower than other groups at 2 and 4 weeks after implantation ($p < 0.05$).
- Significantly higher than other groups at 4 weeks after implantation ($p < 0.05$).

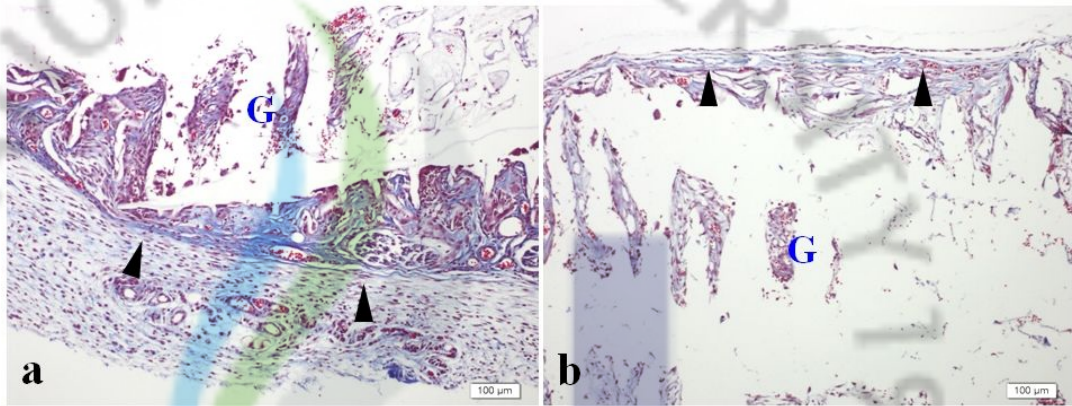


Fig 7. Granulation tissue formation (arrowheads) around graft materials (G) in group CB2 (a) and CBHA (b) at 2 weeks after implantation. Group CB2 showed more thick fibrous tissues and inflammatory reactions than group CBHA. The sections were stained using Masson's trichrome.

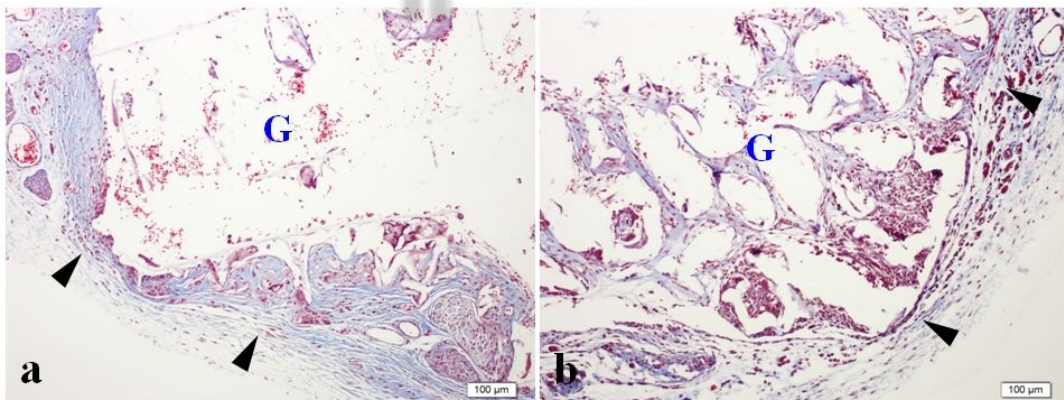


Fig 8. Granulation tissue formation (arrowheads) around graft materials (G) in group CB2 (a) and CBHA (b) at 4 weeks after implantation. Group CB2 still showed thicker fibrous tissues than group CBHA. The sections were stained using Masson's trichrome.

I -4. Discussion

Transformation of CB into CBHA through a hydrothermal reaction process has been widely reported, and CBHA has been confirmed by X-ray diffractometry analysis (Ivankovic *et al.*, 2009, 2010; Kim *et al.*, 2008b; Sivakumar *et al.*, 1996; Wang *et al.*, 2001; Xing *et al.*, 2007). Ivankovic *et al.* (2010) reported that CB was completely transformed into CBHA after 48 h at 200°C. In the present study, CB was completely transformed into the same CBHA, although the conditions of time and temperature were different. It is suggested that the same result can be obtained over the critical time and temperature.

Tissue reactions that are important from the standpoint of biocompatibility mainly relate to an inflammatory reaction (Ryhänen *et al.*, 1998). In this study, inflammatory cells were observed during a 4-week period. Salthouse (1984) reported the response of macrophages to implants; within 24 hours, macrophages were found in close contact with the implant surface. Then, fibroblasts and connective tissue proliferated and, finally, the implant was encapsulated. Butler *et al.* (2001) reported that the thickness of fibrous tissue was widely variable and the fibrous tissue surrounding subcutaneous implants was thinner than that surrounding intraperitoneal ceramic. In this experiment, implantation was inserted subcutaneously. Previous tests of biocompatibility established that more biocompatible implants had thinner surrounding connective tissue (Dupoirieux *et al.*, 2001a; Hwang *et al.*, 1999; Jacob *et al.*, 1998; Lim *et al.*, 2007). Kim *et al.* (2004) reported the same result from mouse abdominal connective tissue. Presently, significantly thinner connective

tissue was observed in the CBHA group ($p < 0.05$). CBHA was confirmed to have higher biocompatibility than CB1, CB2, and CHA. According to Jacob-LaBarre *et al.* (1994) and Dupoirieux *et al.* (2001a), rough-textured surfaces generate thicker capsules, and smooth surfaces usually generate thinner capsules. Superior tissue compatibility should be associated with smooth, well-contoured implants with no acute angles (Salthouse, 1984). The long-term biological response clearly implicates macrophages as the dominant cell type at implant surfaces and that implant stability depends largely on the dynamic behavior of macrophages (Jacob-LaBarre *et al.*, 1994). These observations suggest that the CHA surface is rougher than that of CBHA. This was grossly evident in the present study. Furthermore, group CB2 displayed thinner connective tissue than that of group CB1 2 and 4 weeks later. These results indicate that CB2 preparation is more efficient than that of CB1, albeit no significant difference between them. The thickness of connective tissues tended to be thinner in all groups at 4 weeks. Many researchers have been trying to find out the ideal conditions in the preparation of allograft or xenograft materials. The most generally-used methods are demineralization (Bigham *et al.*, 2008; Begley *et al.*, 1995; Dahners and Jacobs, 1985; Jung *et al.*, 2006; Tuli and Singh, 1978; Um and Him, 1993), freezing (Lee *et al.*, 2007a), freeze-drying (Choung, 1996; Lee *et al.*, 2007a), defat-freezing (Lee *et al.*, 2007a; Song and Lee, 2007), and freeze-drying after defatting (Choi and Lee, 1998; Choung, 1996; Lee *et al.*, 2007a; Song and Lee, 2007). Freezing after defatting confers a higher bone neogenesis effect than freeze-drying after defatting (Choi and Lee, 1998; Choung, 1996; Lee *et al.*, 2007a; Song and Lee, 2007). Specimens processed with freezing after defatting, however, are more limited with respect to transport and storage than freeze-drying after defatting (Lee *et al.*, 2007a).

Also, as described above, the preparation methods associated with allograft and xenograft uniquely involve materials that contain BMP. Bone allograft or xenograft materials containing BMP are reported as being stable when they are processed with freeze-drying after defatting (Choi and Lee, 1998). But, CB is a natural CC ceramic that is different from the implant materials applied in the aforementioned preparation methods. CB1 was processed with freeze-drying after defatting (Fig 1) and CB2 was processed as described previously (Kim *et al.*, 2008b) (Fig 2).

According to the results of Li *et al.* (1999), the ratio of cell components of fibrous capsules changes with the time after implantation. In their study, the population of fibroblasts in fibrous capsules decreased gradually and the population of fibrocytes increased gradually after implantation (Li *et al.*, 1999). Presently, the population changes of fibroblasts and fibrocytes showed a similar trend at 4 weeks after implantation.

Presently, CBHA was the most biocompatible materials among the experimental implants. However, further experiments are necessary to find out more details about the suitable preparation of CB.

The background features a large, faint watermark of the Jeju National University logo. The logo is circular, with the text "JEJU NATIONAL UNIVERSITY" at the top and "제주대학교" at the bottom. In the center, there is a stylized flame or leaf shape in blue, green, and purple, with "JEJU 1952" written below it.

CHAPTER II

Evaluation of the Bone Defect Regeneration
after Implantation with Cuttlebone in Rabbit

II -1. Introduction

Bone regeneration initiated by autogenous cancellous bone occurs by three major steps. First, the undifferentiated osteoprogenitor cells are recruited. Then, by osteoinduction, these cells differentiate to give rise to osteoblasts and chondrocytes. Finally, a suitable scaffold on which active osteoprogenitor cells can produce new bone is established (Gazdag *et al.*, 1995). However, HA and calcium ceramic are not intrinsically osteoinductive (Rose and Oreffo, 2002). Osteoinduction is mediated by numerous growth factors provided by the bone matrix itself. BMP is the typical osteoinductive material. Low molecular weight proteins that initiate endochondral bone formation, presumably by stimulating local progenitor cells of osteoblast lineage and enhancing bone collagen synthesis (Gazdag *et al.*, 1995).

Senn (1889) noted that decalcified bone can induce healing of bone defects. Urist (1965) described ectopic bone induction in intramuscular implantation of decalcified bone. Isolation of the bone-inducing substance revealed a protein that was named BMP (Urist and Strates, 1971).

BMPs are members of the TGF- β superfamily, a large family of secreted factors. The principal activity of BMP is the whole process of embryonic endochondral ossification, but it is ectopic bone induction during postfetal life (Urist, 1965). Recombinant human BMP-2 (rhBMP-2) was the first molecule studied in detail, being produced using Chinese hamster ovary cells (Wang *et al.*, 1990); the authors suggested that this factor would be useful in healing bony defects (Wang, 1993; Wozney, 1998). Moreover, rhBMP-2 increased bone density, bone formation, and callus volume (Bax *et al.*, 1999; Chee *et al.*, 2004; Sykaras *et al.*, 2004; Sykaras *et al.*, 2001; Welch *et al.*, 1998, Yasko *et al.*, 1992). It has been reported that rhBMP-2 in the blood stream is rapidly

diffused (Uludag *et al.*, 2001), and that the osteoinductive potency of rhBMP-2 is significantly increased when it is implanted with a biomaterial scaffold (Uludag *et al.*, 1999; Yokota *et al.*, 2001). Although many potential scaffolds for BMP have been evaluated, suitable scaffolds for BMP have not yet been realized (Rose and Oreffo, 2002; Saito *et al.*, 2001).

Weibrich *et al.* (1998, 2000) compared the surface area of 12 other implants and suggested that the surface area of demineralized bovine bone was 79.7 m²/g. This was five times higher than the surface area of other bone regeneration materials (Weibrich *et al.*, 2000). But, the surface area of CB (386 m²/g) was four times higher than that of demineralized bovine bone. Buffering capacity of CB showed the same pattern as that of CC (Kim *et al.*, 2000). CB is composed of 53.25% Ca, 26.78% O, 14.90% Na, 4.37% Cl, 0.50% Sr, 0.06% P, 0.06% S, and 0.05% Si (Kim *et al.*, 2000). Most of calcium in CB was present in a form of CC. Highly interconnective porosities serve as channels for internal growth of blood vessels and increase bone (Weibrich *et al.*, 2000) and bone containing macro- and micro-pores, which are interconnected to allow necessary body nutrients and fluids to be transported, making bone an extremely complex structure (Ben-Nissan, 2003). Scanning electron microscopy has revealed the multiplayer structure of CB (Birchall and Thomas, 1983; Florek *et al.*, 2009; Kim *et al.*, 2000; Sherrard, 2000; Tiseanu *et al.*, 2005). The minimum pore diameter required for bone ingrowth and angiogenesis into a scaffold is generally considered to be 100 μm (Lu *et al.*, 1999; Nade *et al.*, 1983; Okii *et al.*, 2001). The porous structure diameter of CB is usually between 200 and 600 μm (Birchall and Thomas, 1983), which is similar to cancellous bone (Gu *et al.*, 2009). The optimal osteoconductive pore size for ceramics appears to be between 150 and 500 μm (Flatley *et al.*, 1983). Kim *et al.* (2008b), Lin (1993), and Okumuş and Yildirim (2005) reported that CB represent a new xenograft material in cancellous bone. Until now, there have been no reports on the potency of CB as a xenograft bone substitute in

compact bone studies.

The purpose of this study was to compare bone defect regeneration after implantation of CB in a rabbit calvarial defects model. Bone defect regeneration was measured by radiologic, histologic, and histomorphometric methods.

II-2. Materials and Methods

II-2-1. Fabrication of implants

The CB1, CB2, CBHA, and CHA implants were processed as described in Chapter I. CB1bmp implant was CB1 with rhBMP-2. The rhBMP-2 (rhBMP2[®], Korea Bone Bank, Korea) was produced by a Chinese hamster ovarian cell expression system to yield a glycosylated 26 kilodalton homodimer. rhBMP-2 (100 $\mu\text{g}/\text{cm}^3$) (Itoh et al., 1998) was instilled into CB1 with use of a syringe (fine needle infiltration) at the time of the operation.

II-2-2. Experimental animals and surgical procedure

Twenty seven 9-month-old, 3.2 ± 0.5 kg male New Zealand white rabbits were kept under a standard light-dark schedule and were fed a stock diet and had access to tap water *ad libitum*. The experimental protocol was approved by the Animal Care and Use Committee, Jeju National University (approval number 2010-0042). The rabbits were divided into six groups as shown in Table 2. Aseptic surgical technique was applied during the surgical procedure. They were anesthetized with an intramuscular injection of a dose of tiletamine/zolazepam (Zoletil50[®], Virbac, France). After the anesthesia, incision sites were shaved. The incision sites were then washed with 70% ethanol and scrubbed with 10% povidone iodine. Incision sites were exposed with a sagittal incision through the skin and the periosteum at the midline of the calvaria. With the use of a medical trephine burr (TPHB-B5[®], Osung Mnd, Korea), four standardized full-thickness 5 mm-diameter osseous defects were created in the calvarium of each rabbit under saline irrigation (Figs 9-a, 10-a). In group CB1, CB1bmp, and CHA, the left rostral defect was filled with CB1 disk, the left caudal defect was filled with CB1bmp disk, the right

caudal defect was filled with CHA disk, and the right rostral defect was kept and used as a negative control (Fig 9-b).

In groups CB2 and CBHA, both sides of the rostral and caudal defects were filled with CB2 and CBHA disks (Fig 10-b). The skin was closed with 3-0 nylon. Immediately following implantation, the rabbits were injected subcutaneously with a dose of penicillin G procaine (Combimycin Inj.[®], Green Cross Veterinary Products, Korea) for 3 days.

Table 2. Experimental design for the bone defect regeneration in rabbits

Rabbits	Group	Application	
		Site	Types of implants
n = 18	Blank	R. Ros. Calvaria	Blank
	CHA	R. Cau. Calvaria	CHA
	CB1	L. Ros. Calvaria	CB1
	CB1bmp	L. Cau. Calvaria	CB1 + rhBMP-2
n = 9	CB2	R. Ros. Calvaria	Cuttlebone 2
		L. Ros. Calvaria	Cuttlebone 2
	CBHA	R. Cau. Calvaria	HA from cuttlebone
		L. Cau. Calvaria	HA from cuttlebone

L: Left, R: Right, Ros: Rostral, Cau: Caudal, n: number of experimental animal, CB: Cuttlebone, CHA: Hydroxyapatite from coral, rhBMP-2: Recombinant human bone morphogenetic protein-2

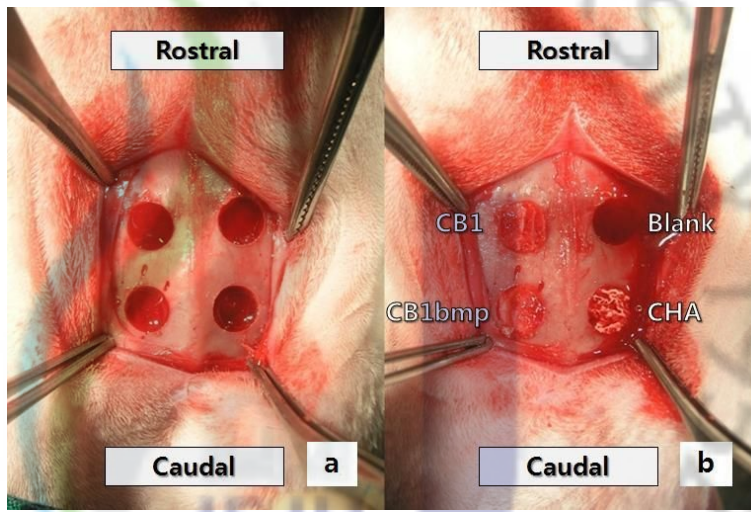


Fig 9. Photographs of rabbit calvarial defect (\varnothing 5 mm) formation (a) and calvarial defects filled with CB1, CB1bmp, and CHA (b).

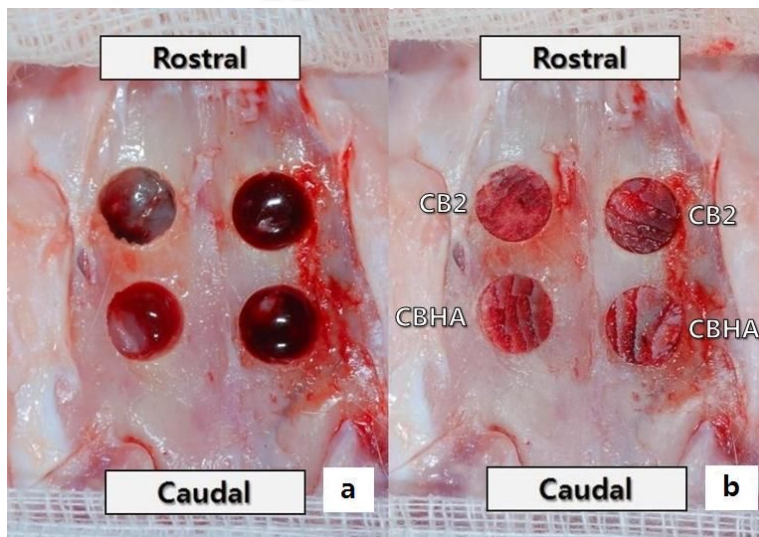


Fig 10. Photographs of rabbit calvarial defect formation (a) and calvarial defects filled with CB2 and CBHA (b).

II-2-3. Radiographic interpretation and radiologic Gray-level histogram (brightness) evaluation

Nine rabbits were euthanized at 4, 8, and 12 weeks postoperatively. The implants and the surrounding calvarial bone were removed. The defect regions were submitted to contact radiography in a dorso-ventral plane with a Kodak Direct View CR975 X-ray System (Eastman Kodak, USA) at an exposure of 42 kVp and 6.4 mAs. Bone formation was evaluated by Gray-level histogram in radiograph processing (Fig 11) using Adobe® Photoshop® 7.0 (Adobe Systems, USA). The histogram of each implant was measured before implantation to calibrate the radiologic Gray-level histogram. Then, the histogram of the implants were measured at 4, 8, and 12 weeks after implantation, and the changes of the histogram were recorded on the basis of a calibrated histogram.

II-2-4. Histologic investigations and histomorphometric analysis

Removed calvarial bone was immersed in 10% phosphate-buffered formalin for 3 days and decalcified for 7 days using 5% formic acid. It was dehydrated in an ethanol series, embedded in paraffin, and cut into 6 mm-thick sections. The sections were stained with H&E stain. The defect closure was determined with a CCD camera-based digital image analysis system (Fig 12). The rate of bone defect regeneration was determined by a histomorphometric method: rate of bone defect regeneration (%) = [(original defect width, mm) - (remained defect width, mm)] / (original defect width, mm) × 100 (Jung *et al.*, 2007; Lee *et al.*, 2008b; Sohn *et al.*, 2010).

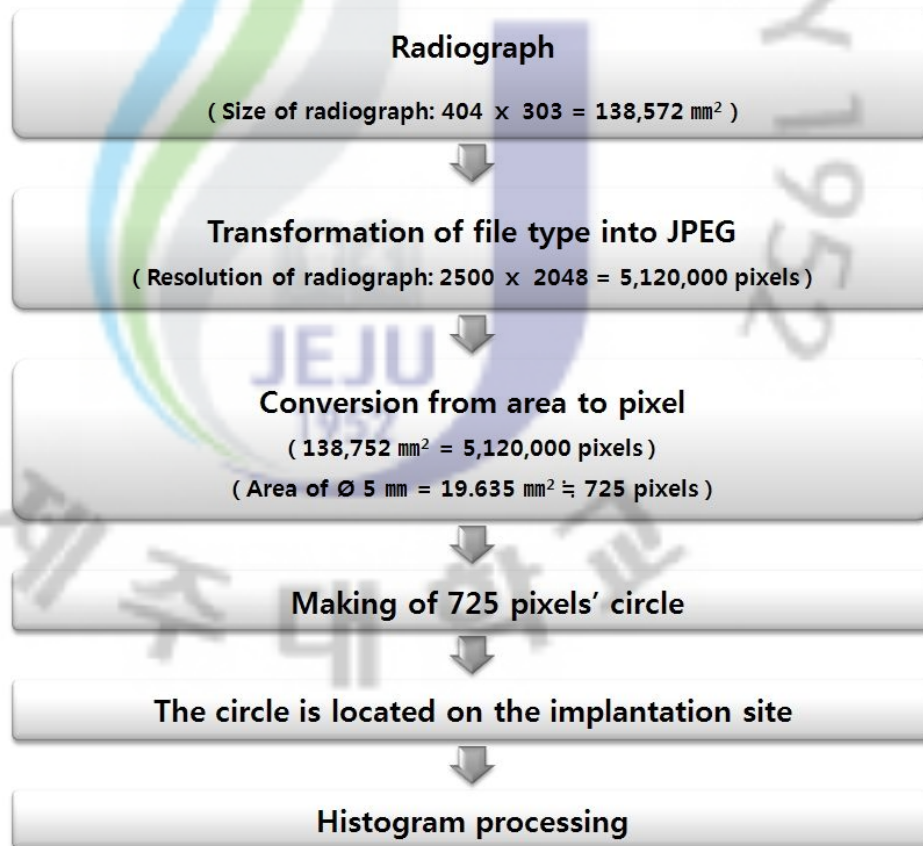
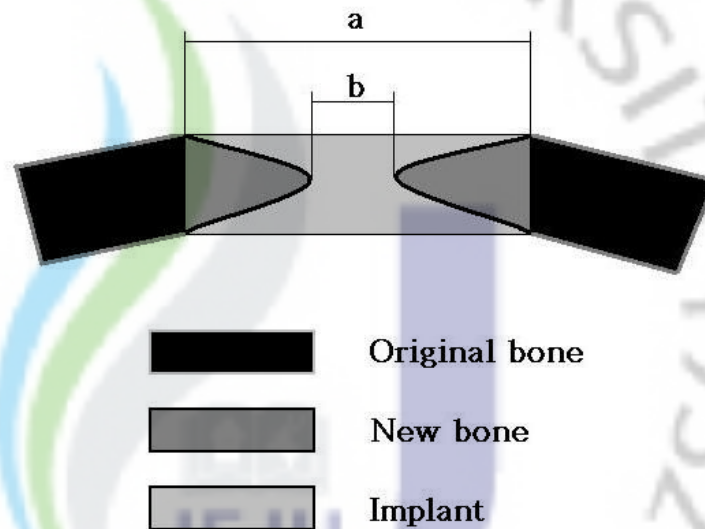


Fig 11. Histogram processing of radiograph by Photoshop program. Radiologic Gray-level histogram was measured to evaluate of bone defect regeneration of each implant 4, 8, and 12 weeks after implantation.



$$\text{The rate of bone defect regeneration (\%)} = (a - b) / a \times 100$$

Fig 12. Measurement of bone defect regeneration in rabbit calvaria by histomorphometric parameters. The measurement was performed 4, 8, and 12 weeks after implantation.

II -2-5. Statistical analysis

The Statistical Package for the Social Science, version 17.0 software (SPSS, USA) was used for data analysis. Mann-Whitney's *u*-test was used to evaluate differences between each group. A *p* value ≤ 0.05 was considered statistically significant.

II-3. Results

II-3-1. Radiologic evaluation

At 4 weeks, in group CB1 and CB1bmp, the radiopaque implant sites were observed. In group CHA, the implant site was more radiopaque than the sites in group CB1 and CB1bmp. In group CB2, partial bone regeneration was observed and the radiopaque implant site was delineated from the surrounding bone by a radiolucent border. In group CBHA, bone regeneration processing towards the centre of the defect was observed and radiopaque implant site was delineated from the surrounding bone by a radiolucent border.

At 8 weeks, the radiopaque implant site in group CB1 revealed a more enlarged circle than group CB1bmp and CHA. In group CB1bmp, a radiopaque implant site was observed and the radiopaque implant site was delineated from the surrounding bone by a radiolucent border. In group CHA, the more radiopaque implant site was observed than group CB1 and CB1bmp. In group CB2, partial bone regeneration was observed and the more enlarged circle was observed than group CBHA. In group CBHA, bone regeneration processing towards the centre of the defect was observed and the radiopaque implant site was delineated partially from the surrounding bone by a radiolucent border.

At 12 weeks, in group CB1 and CB1bmp, partially radiopaque implant sites were observed. In group CHA, a more radiopaque implant site was observed than in groups CB1 and CB1bmp. In group CB2, a radiopaque implant site was observed and the circle was more enlarged than in group CBHA. In group CBHA, bone regeneration processing towards the centre of the defects was observed. At 12 weeks, bone regeneration strikingly advanced in group CBHA comparing with the group CB1, CB2, and CB1bmp.

II -3-2. Total changes of radiologic Gray-level histogram (brightness) during 12 weeks after implantation

In group CBHA, total changes of the radiologic Gray-level histogram was significantly higher than that of the group CHA during 12 weeks after implantation ($p < 0.05$), but there was no significant difference compared with that of the group CB1, CB2, and CB1bmp (Fig 13). In group CHA, total changes of radiologic Gray-level histogram during 12 weeks after implantation was significantly lower than that of the other groups ($p < 0.05$) (Fig 13). In group CB1, CB2, CB1bmp, and CBHA, total changes of the radiologic Gray-level histograms were similarly changed during the 12 weeks, but there was no significant difference compared with that of the other groups (Fig 13). At 12 weeks, group CHA was significantly lower than that of the other group ($p < 0.05$) (Fig 13). This evaluation was calibrated as the numerical value.

II -3-3. Histomorphometric analysis for bone defect regeneration

The rate of bone defect regeneration of the implanted site in group CHA was significantly higher than that of other groups at 4 and 8 weeks after implantation ($p < 0.05$) (Fig 14). At 12 weeks, the rate of bone defect regeneration in group CHA was significantly higher than that of group CB1, CB2, and CB1bmp ($p < 0.05$). But, there were no significant differences between group CHA and CBHA (Fig 14).

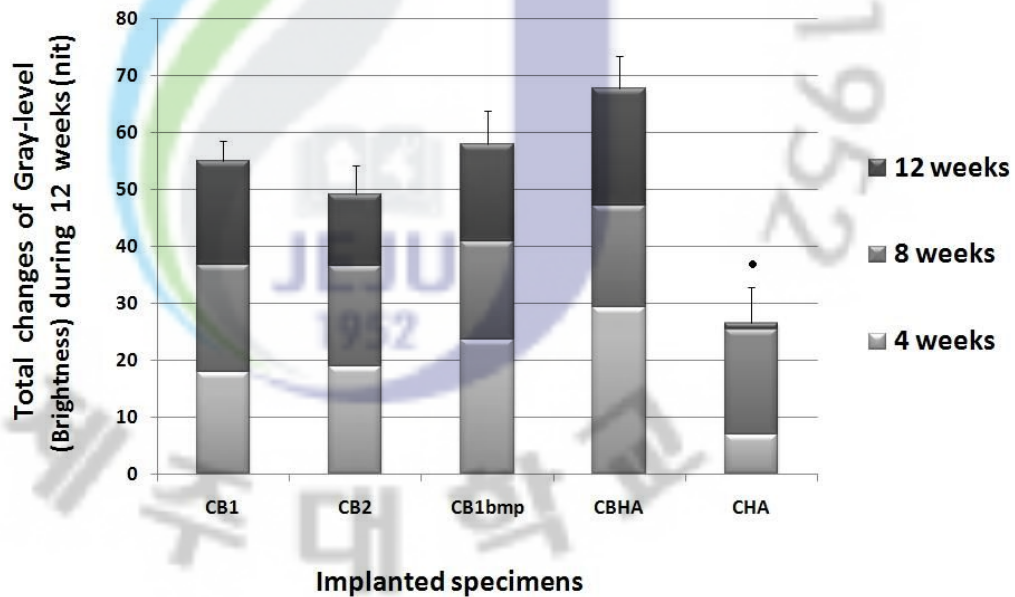


Fig 13. Total 12-week changes of radiologic Gray-level histogram in each specimen. The change of Gray-level histogram in group CBHA was the highest after implantation, but there were no significant differences between group CB1 and CB1bmp. Values expressed as mean \pm SE.

- Significantly lower than other groups after implantation ($p < 0.05$).

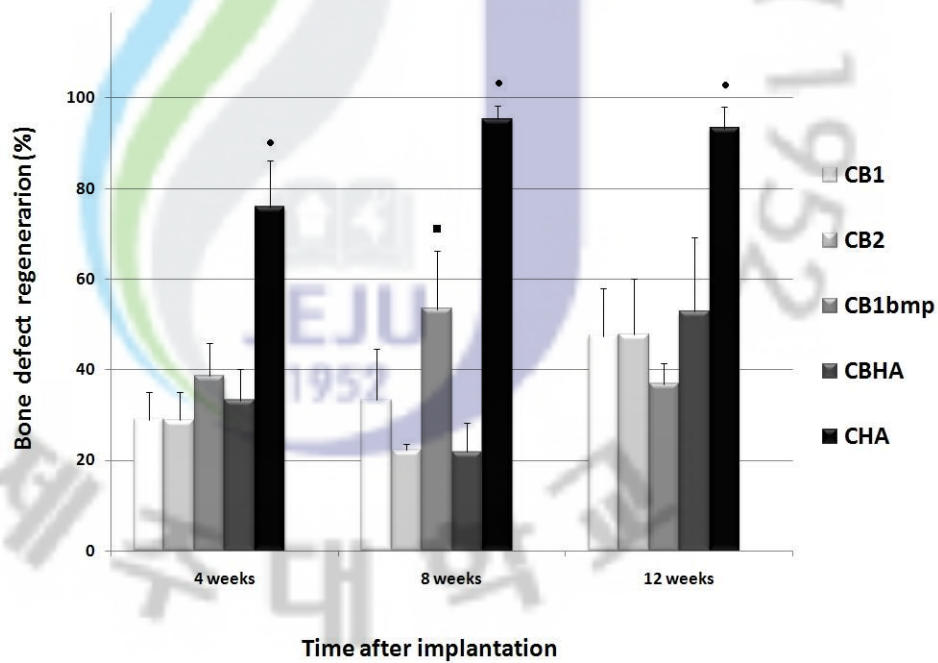


Fig 14. The rate of bone defect regeneration group CB1, CB2, CB1bmp, CBHA, and CHA specimens. Values are expressed as mean \pm SE.

- Significantly higher than other groups at 4, 8, and 12 weeks after implantation ($p < 0.05$).
- Significantly higher than group CBHA at 8 weeks after implantation ($p < 0.05$).

II -3-4. Histologic evaluation

At 4 weeks after implantation, all graft materials in the calvarial defect area were surrounded by moderate to severe dense fibrous collagenous fibers (Fig 15). Multifocal to diffuse inflammation composed of neutrophils, macrophages, and foreign body giant cells were scattered in the adjacent area of fibrous tissues. In the CHA group, proliferated collagenous fibers were invaginated into the graft materials.

At 8 weeks after implantation, overall fibrous stromal reaction in each group was gradually increased, as compared to 4 weeks. However, the inflammatory reaction was dramatically decreased. Compared with other groups, most graft materials were replaced by inward growing new bone in group CHA.

At 12 weeks after implantation, variable extents of bone growth into defect areas were observed in all experimental groups (Fig 16). New bone formation extended into graft materials in group CBHA and CHA (Fig 17). However, fibrous stromal and inflammatory reactions still remained in groups CB1, CB1bmp, CB2, but little remained in groups CBHA and CHA. In group CHA, an obvious continuity of cortical bone from the calvaria was observed in both sides of the bone defect. A marked increased number of osteoblasts were present at the surface of bonny spicules. Multifocal bone marrow formation also existed in cortical bone (Figs 16, 17).

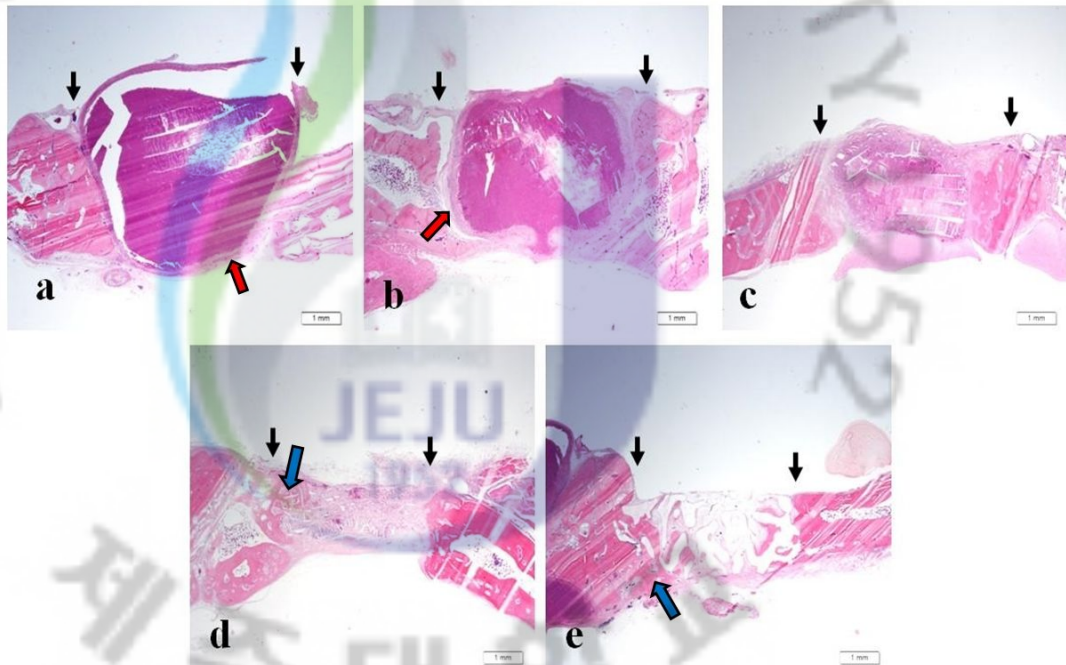


Fig 15. Histologic sections of group CB1 (a), CB1bmp (b), CB2 (c), CBHA (d), and CHA (e) at 4 weeks after implantation (black arrows: defect margins). Group CB1 and CB1bmp were encapsulated by fibrous connective tissue (a, b: red arrows). Bone defect regeneration was observed at defect margins in group CBHA and CHA (d, e: blue arrows). The sections were stained using H&E.

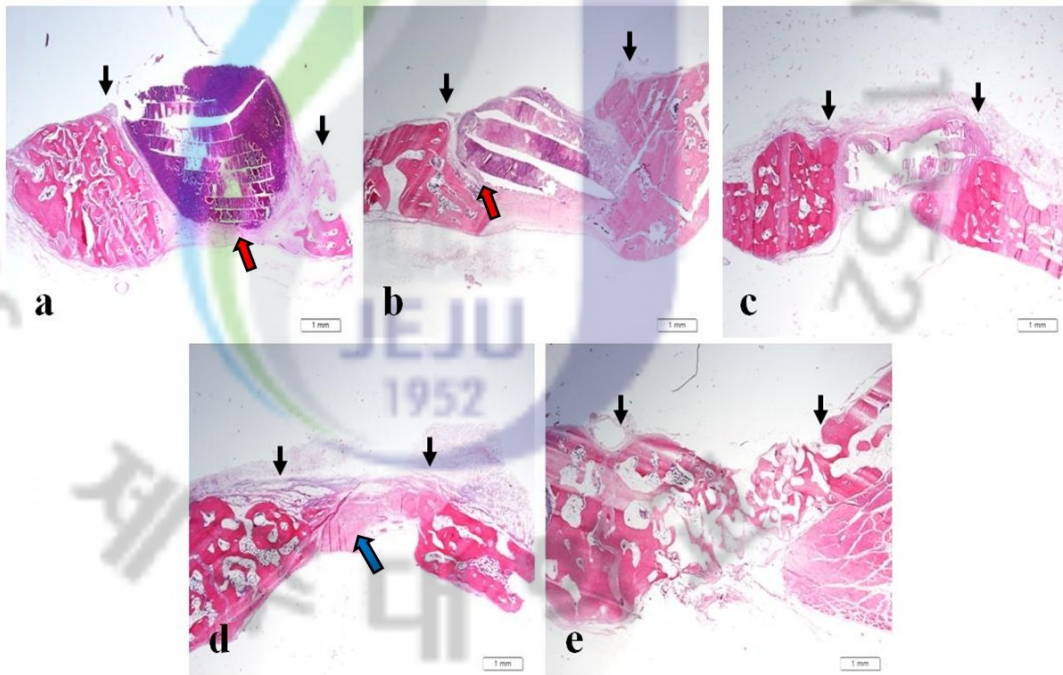


Fig 16. Histologic sections of group CB1 (a), CB1bmp (b), CB2 (c), CBHA (d), and CHA (e) at 12 weeks after implantation (black arrows: defect margins). CB1 and CB1bmp implants were still encapsulated by thick fibrous connective tissue (a, b: red arrows). New bone formation was observed in group CBHA (d: blue arrow). The sections were stained using H&E.

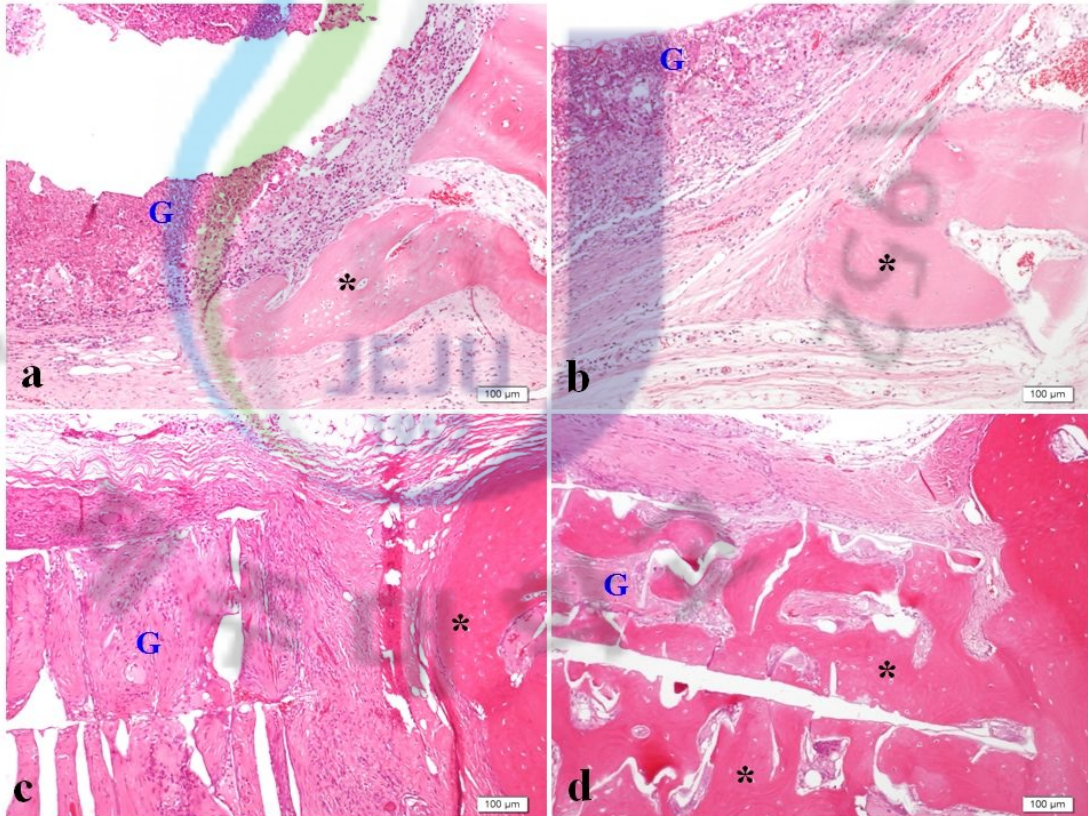


Fig 17. Histologic features of new bone formation in group CB1 (a), CB1bmp (b), CB2 (c), and CBHA (d) at 12 weeks after implantation. New bone formation (asterisks) was observed around the graft material (G) in group CB1 or CB1bmp and inside of graft material in group CBHA. The sections were stained using H&E.

II-4. Discussion

Sohn *et al.* (2010) reported that the critical size defect was not suggested in a rabbit calvarial model. Huh *et al.* (2005) suggested that the critical size defect depends on the presence of the periosteum. A defect with a diameter of 5 mm is a commonly used size in rat models (Lee *et al.*, 2008a; Dupoirieux *et al.*, 1995). Presently, considering the convenience of operation, defects with a diameter of 5 mm were created in the calvaria of rabbits and the periosteum surrounding the implant was widely-removed.

Interconnecting pores are the pathway for new vessels, which is an advantage for new bone formation (Okii *et al.*, 2001). Blood supply to the cancellous bone is much better than to the compact bone. For this reason, bone regeneration in cancellous bone is faster than in compact bone. Nevertheless, this study was performed to the compact bone, in order to directly observe the bone defect regeneration without cartilage formation.

Itoh *et al.* (1998) reported that the lowest dose of rhBMP-2 needed for defect healing was between 40 and 160 $\mu\text{g}/\text{cm}^3$ and suggested a 100 $\mu\text{g}/\text{cm}^3$ dose, based on results in canine ulnar defect model. In this study, the dose of rhBMP-2 was 100 $\mu\text{g}/\text{cm}^3$ (Itoh *et al.*, 1998). From the results, we decided that the dose of rhBMP-2 in CB was suitable or not, because this study was not focused on the determination of dose of rhBMP-2. But the dose of 100 $\mu\text{g}/\text{cm}^3$ was effective in bone defect regeneration.

In bone defect regeneration, radiologic analysis is commonly used to compare the feasibility of bone graft use in different studies (Dupoirieux *et al.*, 1995; Durmuş *et al.*, 2007; Itoh *et al.*, 1998; Karaismailoğlu *et al.*, 2002). In group

CHA, a more radiopaque implant site was observed than apparent in the surrounding bone and the other groups at 12 weeks after implantation. Bone regeneration was determined by changes of radiodensity. For this reason, bone regeneration processing of CHA implant could not be observed during 12 weeks after implantation. But, 8 and 12 weeks after implantation, an ill-defined change was apparent between bone and implant, indicating that bone remodeling occurred in the CHA group. This finding is same result with other studies (Dupoirieux *et al.*, 1999; Durmuş *et al.*, 2007). In group CB1, the size of defect was enlarged at 8 weeks after implantation.

This osteolysis is thought to be immune responses. In this study, this foreign body reaction can be found in the biocompatibility test of CB1. A similar observation was reported by Durmuş *et al.* (2007). In the latter study, an excessive foreign body reaction characteristic of encapsulation was evident. Karaismailoğlu *et al.* (2002), suggested that xenografts still have some disadvantages in terms of graft incorporation, resorption, mechanical strength, and other problems linked to immunologic rejection and microbiologic contamination. Presently, groups CB1 and CB1bmp were encapsulated with a dense fibrous tissue with inflammatory cells such as neutrophils, macrophages, and foreign body giant cells at 4, 8, and 12 weeks after implantation. For this inflammatory reaction, freeze-drying after defatting was not suitable for CB.

In group CBHA, the most visible bone regeneration processing towards the centre of the defect was observed. The biocompatibility of CBHA echoes the findings of another study (Chiroff *et al.*, 1975).

In the study of Zegzula *et al.* (1997), Gray-level density was measured on the basis of the standard radiographs, and the percentage of radiopacity was determined with a computer algorithm that divides the radiopaque area of the

defect by the total area of the measuring frame. Presently, the radiologic Gray-level histogram was measured for objective assessment of the radiologic findings using a similar principle. The Gray-level histogram change in group CBHA during 12 weeks was the highest, indicating that bone regeneration in this group is most active, corroborating the results of radiologic analysis. However, there was no significant difference in the Gray-level histogram changes between groups CB1 and CB1bmp during 12 weeks. Evaluation of bone defect regeneration was measured objectively by Gray-level histogram. The result supported that of a previous study (Zegzula, 1997).

To confirm the bone regeneration capacity, the defect closure of each group was measured 4, 8, and 12 weeks after implantation. The measurement of defect closure has been used before (Jung *et al.*, 2007; Lee *et al.*, 2008b). According to the results of Kim *et al.* (2008a), the amount of newly-matured bone in the implanted material with rhBMP-2 was more than that evident without rhBMP-2. In this study, after 8 weeks, group CB1bmp showed significantly higher result than group CBHA ($p < 0.05$). It is considered that the rhBMP-2 played a critical role in bone regeneration, but CB1 did not participate as the scaffold of rhBMP-2, considering the thickness of connective tissue. It is considered that rhBMP-2 contained in CB1 was freed to the surrounding bone tissue where it promoted the bone regeneration, but rhBMP-2 did not spread to the other implant sites. Regarding overall changes of defect closure, the bone regeneration capacity of CHA was the highest, followed by CBHA. Because this measurement of bone defect regeneration is invasive, the radiologic Gray-level histogram will be a valuable method in clinical use. Advantages of CB and CBHA include their ready availability, inexpensive cost, unlimited quantity and soft-textured surface. However, they suffer from weak strength. Conversely, CB and CBHA are easy to process

and are suitable for use in irregular bone defects like sealing bone wax. Considering the biocompatibility of CBHA, the possibility that BMP acts as a scaffold is expected. Furthermore, CBHA will be able to be used by carrier or scaffold in stem cells. It was inconvenient not to have a study of CB2 + rhBMP-2.

Ideal bone substitutes should be resorbed with time and replaced by newly formed bone (Park *et al.*, 2008). In this study, newly formed bones and bone resorption were observed inside of graft material in group CBHA 12 weeks after implantation. But, there was no new bone formation in groups CB1, CB1bmp, and CB2. It is considered that the CBHA is a more biocompatible material in compact bone defect regeneration than CB1, CB1bmp, and CB2. However, further experiments are necessary to find out in more detail about the suitable absorptivity of CBHA.

To apply the most effective scaffold of bone graft substitute, various preparations of CB and different types (such as powder, paste, granule) of CBHA implantation should be studied.

CONCLUSIONS

This study was conducted to evaluate the biocompatibility of CB1, CB2, CBHA, and CHA using a mouse subcutaneous implant model and bone defect regeneration with CB1, CB2, CB1bmp, CBHA, and CHA in a rabbit calvarial defects model. The efficiency was compared with other commonly used CHA. The findings of this study indicate that CBHA is a safer material for use inside the body than CHA. CBHA has a more effective osteoconduction than CB1, CB1bmp, and CB2. CBHA is a valuable bone graft material in compact bone defect models.

REFERENCES

- Aalto M, Heppleston AG. Fibrogenesis by mineral fibres: an in-vitro study of the roles of the macrophage and fibre length. *Br J Exp Pathol* 1984; 65(1): 91-99.
- Bakker D, van Blitterswijk CA, Hesselink SC, Grote JJ. Effect of implantation site on phagocyte/polymer interaction and fibrous capsule formation. *Biomaterials* 1988; 9(1): 14-23.
- Bax BE, Wozney JM, Ashhurst DE. Bone morphogenetic protein-2 increases the rate of callus formation after fracture of the rabbit tibia. *Calcif Tissue Int* 1999; 65: 83-89.
- Begley CT, Doherty MJ, Mollan RAB, Wilson DJ. Comparative study of the osteoinductive properties of bioceramic, coral and processed bone graft substitutes. *Biomaterials* 1995; 16: 1181-1185.
- Behling CA, Spector M. Quantitative characterization of cells at the interface of long-term implants of selected polymers. *J Biomed Mater Res* 1986; 20(5): 653-666.
- Ben-Nissan B. Natural bioceramics: from coral to bone and beyond. *Curr Opin Solid State Mat Sci* 2003; 7: 283-288.
- Bigham AS, Dehghani SN, Shafiei Z, Nezhad ST. Xenogenic demineralized bone matrix and fresh autogenous cortical bone effects on experimental

bone healing: radiologic, histopathologic and biomechanical evaluation. J Orthopaed Traumatol 2008; 9: 73-80.

Birchall JD, Thomas NL. On the architecture and function of cuttlefish bone. Journal of materials science 1983; 18: 2081-2086.

Bosch C, Melsen B, Karin V. Guided bone regeneration in calvarial bone defects using polytetrafluoroethylene membranes. Cleft Palate-Craniofacial Journal 1995; 32(4): 311-317.

Butler K, Benghuzzi H, Puckett A. Cytological evaluation of the tissue-implant reaction associated with S/C and I/P implantation of ALCAP and HA bioceramics *in vivo*. Pathol Res Pract 2001; 197: 29-39.

Carson JS, Bostrom MP. Synthetic bone scaffolds and fracture repair. Injury 2007; 38(S1): S33-S37.

Chee YD, Oh SH, Min SK, Keon KH, Lee KS. Effect of bone morphogenetic protein on a rabbit mandibular distraction osteogenesis. J Korean Assoc Maxillofac Plast Reconstr Surg 2004; 26(2): 137-150.

Chiroff RT, White EW, Weber JN, Roy DM. Tissue ingrowth of replamineform implants. J Biomed Mater Res 1975; 9(4): 29-45.

Choi IH, Lee CI. Effectiveness of transplantation by freeze-dried bone of goat to dogs. Korean J Vet Clin Med 1998; 15(2): 442-449.

Choi IH, Lee MJ, Choi OK, Joung IS, Choi SJ, Kim NS. Changes of xenograft according to extracted time with chloroform-methanol solution

in freeze-dried cortical bone of pig transplanted to dogs. J Vet Clin 2003; 20(1): 91-95.

Chou J, Ben-Nissan B, Choi AH, Wuhrer R, Green D. Conversion of coral sand to calcium phosphate for biomedical applications. J Aust Ceram Soc 2007; 43(1): 44-48.

Choung PH. An experimental study of undemineralized freeze-dried human bone. J Korean Assoc Maxillofac Plast Reconstr Surg 1996; 18(1): 164-174.

Clark AE, Hench LL, Paschall HA. The influence of surface chemistry on implant interface histology: A theoretical basis for implant materials selection. J Biomed Mater Res 1976; 10(3): 161-174.

Dahners LE, Jacobs RR. Long bone defects treated with demineralized bone. Southern Medical Journal 1985; 78(8): 933-934.

Dupoirieux L, Pourquier D, Neves M, Téot L. Resorption kinetics of eggshell: An *in vivo* study. J Craniofac Surg 2001a; 12(1): 53-58.

Dupoirieux L, Pourquier D, Picot MC, Neves M. Comparative study of three different membranes for guided bone regeneration of rat cranial defects. Int J Oral Maxillofac Surg 2001b; 30: 58 - 62.

Dupoirieux L, Pourquier D, Picot MC, Neves M. The effect of pentosan polysulphate on bone healing of rat cranial defects. J Craniomaxillofac Surg 1999; 27: 314-320.

Dupoirieux L, Pourquier D, Souyris F. Powdered eggshell: a pilot study on a new bone substitute for use in maxillofacial surgery. *J Craniomaxillofac Surg* 1995; 23: 187-194.

Durmuş E, Çelik I, Aydın MF, Yıldırım G, Sur E. Evaluation of the biocompatibility and osteoproliferative activity of ostrich eggshell powder in experimentally induced calvarial defects in rabbits. *J Biomed Mater Res Part B: Appl Biomater* 2007; 86B: 82 - 89.

Finkemeier CG. Current concepts review bone-grafting and bone-graft substitutes. *J Bone Joint Surg Am* 2002; 84(4): 454-464.

Flatley TJ, Lynch KL, Benson M. Tissue response to implants of calcium phosphate ceramic in the rabbit spine. *Clin Orthop Relat Res* 1983; 179: 246-252.

Florek M, Fornal E, Gómez-Romero P, Zieba E, Paszkowicz W, Lekki J, Nowak J, Kuczumow A. Complementary microstructural and chemical analyses of *Sepia officinalis* endoskeleton. *Mater Sci Eng C* 2009; 29(4): 1220-1226.

Froum SJ, Weinberg MA, Tarnow D. Comparison of bioactive glass synthetic bone graft particles and open debridement in the treatment of human periodontal defects. *J Periodontol* 1998; 69(6): 698-709.

Gazdag AR, Lane JM, Glaser D, Forster A. Alternatives to autogenous bone graft: efficacy and indications. *J Am Acad Orthop Surg* 1995; 3: 1-8.

Gu SJ, Sohn JY, Lim HC, Um YJ, Jung UW, Kim CS, Lee YK, Choi SH, The effects of bone regeneration in rabbit calvarial defect with particulated and block type of hydroxyapatite. J Korean Acad Periodontol 2009; 39: 321-329.

Guillemin G, Patat JL, Fournie J, Chetail M. The use of coral as a bone graft substitute. J Biomed Mater Res 1987; 21(5): 557-567.

Holmes R, Mooney V, Bucholz R, Tencer A. A coralline hydroxyapatite bone graft substitute. Clin Orthop Relat Res 1984; 188: 252-262.

Huh JY, Choi BH, Kim BY, Lee SH, Zhu SJ, Jung JH. Critical size defect in the canine mandible. Oral Surg Oral Med Oral Pathol Oral Radiol Endod 2005; 100(3): 296-301.

Hwang SK, Lee KC, Rhim KH. Biocompatibility of biodegradable film by natural polymers. J Korean Ind Eng Chem 1999; 10(6): 939-943.

Ilan DI, Ladd AL. Bone graft substitutes. Plast Reconstr Surg 2003; 9(4): 151-160.

Ivankovic H, Ferrer GG, Tkalcec E, Orlic S, Ivankovic M. Preparation of highly porous hydroxyapatite from cuttlefish bone. J Mater Sci: Mater Med 2009; 20: 1039-1046.

Ivankovic H, Tkalcec E, Orlic S, Ferrer GG, Schauerl Z. Hydroxyapatite formation from cuttlefish bones: kinetics. J Mater Sci Mater Med 2010; 21(10): 2711-2722.

Itoh T, Mochizuki M, Nishimura R, Matsunaga S, Kadosawa T, Kokubo S, Yokota S, Sasaki N. Repair of ulnar segmental defect by recombinant human bone morphogenetic protein-2 in dogs. J Vet Med Sci 1998; 60(4): 451-458.

Jacob JT, Burgoyne CF, McKinnon SJ, Tanji TM, LaFleur PK, Duzman E. Biocompatibility response to modified baerveldt glaucoma drains. J Biomed Mater Res 1998; 43(2): 99-107.

Jacob - LaBarre JT, Assouline M, Byrd T, McDonald M. Synthetic scleral reinforcement materials: I. Development and *in vivo* tissue biocompatibility response. J Biomed Mater Res 1994; 28(6): 699 - 712.

Johnson AL, Hulse DA. Fundamentals of orthopedic surgery and fracture management. In: Small animal surgery, 2nd ed. USA: Mosby. 2002: 821-893.

Jung SW, Jung JH, Chae GJ, Jung UW, Kim CS, Cho KS, Chai JK, Kim CK, Choi SH. The analysis of bone regenerative effect with carriers of bone morphogenetic protein in rat calvarial defects. J Korean Acad Periodontol 2007; 37(4): 733-742.

Jung YH, Nah KS, Cho BH. Change of the fractal dimension according to the decalcification degree and the exposure time in the bovine rib. Korean J Oral Maxillofac Radiol 2006; 36: 69-72.

Karaismailoğlu TN, Tomak Y, Andaç A, Ergün E. Comparison of autograft, coralline graft, and xenograft in promoting posterior spinal fusion. Acta Orthop Traumatol Turc 2002; 36(2): 147-154.

Kim CB, Lee MH, Kim BI, Min BW, Kim MH, Choe ES, Cho HW. Comparative biocompatibility of metal implants in connective tissue of abdominal wall of the mouse. *J Toxicol Pub Health* 2004; 20(1): 13-20.

Kim DJ. Autogenous bone graft and bone substitutes. *J of Korean Spine Surg* 2008; 15(1): 54-65.

Kim HS, Lee MY, Lee SC. Characteristics of sepiae os as a calcium source. *J Korean Soc Food Sci Nutr* 2000; 29(4): 743-746.

Kim JH, Kim CH, Kim KW. Bone healing capacity of the collagen bone filler (TERUPLUG[®]) and rhBMP-2 in rabbit cranium defect. *J Kor Oral Maxillofac Surg* 2008a; 34: 119-130.

Kim, JJ, Kim HJ, Lee KS. Evaluation of biocompatibility of porous hydroxyapatite developed from edible cuttlefish bone. *Key Engineering Materials* 2008b; 361(363): 155-158.

Kim TI. A histomorphometric study of bone apposition to newly developed Ti-based alloys in rabbit bone. *J Korean Acad Prosthodont* 1998; 36(5): 701-720.

Lee CH, Jang JH, Lee JM, Suh JY, Park JW. Histomorphometric evaluation of bone healing with natural calcium carbonate derived bone substitute in rat calvarial defect. *J Korean Acad Periodontol* 2008a; 38: 83-90.

Lee JI, Song HN, Kim NS, Choi IH. Comparison of osteoinductive effect of freezing, freeze-drying and defat-freezing implant preparation for allograft in rabbit. *Korean J Vet Res* 2007a; 47(2): 219-228.

Lee SJ, Yoon YS, Lee MH, Oh NS. Highly sinterable β -tricalcium phosphate synthesized from eggshells. Mater Lett 2007b; 61: 1279-1282.

Lee SK, Kim JS, Kang EJ, Eum TK, Kim CS, Cho KS, Chai JK, Kim CK, Choi SH. Effects of rhBMP-2 with various carriers on bone regeneration in rat calvarial defect. J Korean Acad Periodontol 2008b; 38: 125-134.

Lee YM, Lee EJ, Yeom DS, Kim DS, Yee ST, Kim BI, Cho HW. Relative Biocompatibility Evaluation of Anodized Titanium Specimens *in vivo* and *in vitro*. J Life Science 2006; 16(2): 302-309.

LeGeros RZ. Properties of osteoconductive biomaterials: calcium phosphates. Clin Orthop Relat Res 2002; 395: 81-98.

Lehle K, Lohn S, Reinerth G, Schubert T, Preuner JG, Birnbaum DE. Cytological evaluation of the tissue-implant reaction associated with subcutaneous implantation of polymers coated with titaniumcarboxonitride *in vivo*. Biomaterials 2004; 25(24): 5457-5466.

Li DJ, Ohsaki K, Li K, Cui PC, Ye Q, Baba K, Wang QC, Tenshin A, Takano-Yamamoto T. Thickness of fibrous capsule after implantation of hydroxyapatite in subcutaneous tissue in rats. J Biomed Mater Res 1999; 45: 322-326.

Lim HC, Chae GJ, Jung UW, Kim CS, Lee YK, Cho KS, Kim CK, Choi SH. Initial tissue response of biodegradable membrane in rat subcutaneous model. J Korean Acad Periodontol 2007; 37(4): 839-848.

Lin S. The preparation of cuttlebone/bone morphogenetic protein composite and the experimental study on its action of osteoinduction. Chinese J Trad Med Traumatol Orthoped 1993; 4: 1-4.

Lu JX, Flautre B, Anselme K, Hardouin P, Gallur A, Descamps M, Thierry B. Role of interconnections in porous bioceramics on bone recolonization *in vitro* and *in vivo*. J Mater Sci Mater Med 1999; 10: 111-120.

Macedo NL, Matuda FS, Macedo LGS, Gonzalez MB, Ouchi SM, Carvalho YR. Bone defect regeneration with bioactive glass implantation in rats. J Appl Oral Sci 2004; 12(2): 137-143.

Mastrogiacomo M, Muraglia A, Komlev V, Peyrin F, Rustichelli F, Crovace A, Cancedda R. Tissue engineering of bone: search for a better scaffold. Orthod Craniofacial Res 2005; 8: 277-284.

Matlaga BF, Yassenchak LP, Salthouse TN. Tissue response to implanted polymers: The significance of sample shape. J Biomed Mater Res 1976; 10(3): 391-397.

Millis DL, Martinez SA. Bone graft. In: Textbook of small animal surgery, 3rd ed. Philadelphia: Saunders. 2002: 1875-1891.

Nade S, Armstrong L, McCartney E, Baggaley B. Osteogenesis after bone and bone marrow transplantation. The ability of ceramic materials to sustain osteogenesis from transplanted bone marrow cells: preliminary studies. Clin Orthop Relat Res 1983; 181: 255-263.

Okii N, Nishimura S, Kurisu K, Takeshima Y, Uozumi T. In vivo histological changes occurring in hydroxyapatite cranial reconstruction. *Neurol Med Chir* 2001; 41: 100-104.

Okumuş Z, Yildirim ÖS. The cuttlefish backbone: A new bone xenograft material?. *Turk J Vet Anim Sci* 2005; 29: 1177-1184.

Park JW, Bae SR, Suh JY, Lee DH, Kim SH, Kim H, Lee CS. Evaluation of bone healing with eggshell-derived bone graft substitutes in rat calvaria: A pilot study. *J Biomed Mater Res* 2008; 87A: 203 - 214.

Park JW, Jang JH, Bae SR, An CH, Suh JY. Bone formation with various bone graft substitutes in critical-sized rat calvarial defect. *Clin Oral Impl Res* 2009; 20: 372-378.

Piermattei DL, Flo GL. Bone grafting. In: *Handbook of small animal orthopedics and fracture repair*, 3rd ed. Philadelphia, London, Toronto, Montreal, Sydney, Tokyo: WB Saunders Co. 1997: 147-153.

Rose FR, Oreffo RO. Bone tissue engineering: Hope vs Hype. *Biochem Biophys Res Commun* 2002; 292: 1-7.

Roy DM, Linnehan SK. Hydroxyapatite formed from Coral Skeletal Carbonate by Hydrothermal Exchange. *Nature* 1974; 247: 220-222.

Ryhänen J, Kallioinen M, Tuukkanen J, Junila J, Niemelä E, Sandvik P, Serlo W. *In vivo* biocompatibility evaluation of nickel-titanium shape memory metal alloy: Muscle and perineural tissue responses and capsule membrane thickness. *J Biomed Mater Res* 1998; 41: 481-488.

Ryu SY, Park SC, Yun CJ. The effect of bioactive glass and resorbable membrane on bone regeneration of the mandibular bone defects in rabbit. *J Korean Assoc Oral Maxillofac Surg* 2000; 26(6): 613-619.

Saito N, Okada T, Horiuchi H, Murakami N, Takahashi J, Nawata M, Ota H, Nozaki K, Takaoka K. A biodegradable polymer as a cytokine delivery system for inducing bone formation. *Nat Biotechnol* 2001; 19: 332-335.

Salthouse TN. Some aspects of macrophage behavior at the implant interface. *J Biomed Mater Res* 1984; 18(4): 395-401.

Senn N. Senn on the healing of aseptic bone cavities by implantation of antiseptic decalcified bone. *Ann Surg* 1889; 10(5): 352-368.

Sherrard KM. Cuttlebone morphology limits habitat depth in eleven species of sepia (Cephalopoda: Sepiidae). *Biol Bull* 2000; 198: 404-414.

Sivakumar M, Kumart TSS, Shantha KL, Rao KP. Development of hydroxyapatite derived from Indian coral. *Biomaterials* 1996; 17: 1709-1714.

Sohn JY, Park JC, Um YJ, Jung UW, Kim CS, Cho KS, Choi SH. Spontaneous healing capacity of rabbit cranial defects of various sizes. *J Periodontal Implant Sci* 2010; 40: 180-187.

Song HN, Lee JI. Comparison of efficacy of new bone formation according to implant treatment in xenograft transplanted for experimental bone defects of rabbit. *J Vet Clin* 2007; 24(3): 350-357.

Stevenson S. The immune response to osteochondral allograft in dogs. *J Bone Joint Surg Am* 1987; 69: 573-582.

Sykaras N, Iacopino AM, Triplett RG, Marker VA. Effect of recombinant human bone morphogenetic protein-2 on the osseointegration of dental implants: a biomechanics study. *Clin Oral Invest* 2004; 8: 196-205.

Sykaras N, Triplett RG, Nunn ME, Iacopino AM, Opperman LA. Effect of recombinant human bone morphogenetic protein-2 on bone regeneration and osseointegration of dental implants. *Clin Oral Impl Res* 2001; 12: 339 - 349.

Tadic D, Epple M. A thorough physicochemical characterisation of 14 calcium phosphate-based bone substitution materials in comparison to natural bone. *Biomaterials* 2004; 25: 987-994.

Tiseanu I, Craciunescu T, Mandache NB, Duluiu OG. μ -X-Ray computer axial tomography application in life sciences. *Journal of optoelectronics and advanced materials* 2005; 7(2): 1073-1078.

Tuli SM, Singh AD. The osteoninductive property of decalcified bone matrix. *J Bone Joint Surg Am* 1978; 60(B): 116-123.

Uludag H, D'Augusta D, Palmer R, Timony G, Wozney JM. Characterization of rhBMP-2 pharmacokinetics implanted with biomaterial carriers in the rat ectopic model. *J Biomed Mater Res* 1999; 46: 193-202.

Uludag H, Gao T, Porter TJ, Friess W, Wozney JM. Delivery systems for BMPs: factors contributing to protein retention at an application site. *J Bone Joint Surg Am* 2001; 83(1): S128-S135.

Um IW, Him EC. Experimental study on the influence of HCL concentration on the healing process of allogeneic bone graft. J Korean Assoc Maxillofac Surg 1993; 19(2): 217-225.

Urist MR. Bone: Formation by autoinduction. Science 1965; 150(3698): 893-899.

Urist MR, Strates BS. Bone morphogenetic protein. J Dent Res 1971; 50: 1392-1406.

Vuola J, Böhling T, Kinnunen J, Hirvensalo E, Asko-Seljavaara S. Natural coral as bone-defect-filling material. J Biomed Mater Res 2000; 51: 117-122.

Vuola J, Göransson H, Böhling T, Asko-Seljavaara S. Bone marrow induced osteogenesis in hydroxyapatite and calcium carbonate implants. Biomaterials 1996; 17: 1761-1766.

Vuola J, Taurio R, Göransson H, Asko-Seljavaara S. Compressive strength of calcium carbonate and hydroxyapatite implants after bone-marrow-induced osteogenesis. Biomaterials 1998; 19: 223-227.

Walsh WR, Morberg P, Yu Y, Yang JL, Haggard W, Sheath PC, Svehla M, Bruce WJM. Response of a calcium sulfate bone graft substitute in a confined cancellous defect. Clin Orthop Relat Res 2003; 406: 228-236.

Wang DZ, Liu JH, Chen QW. Study on cuttlebone modified to hydroxyapatite and its nanoscale microstructure. Rare Metal Mat Engin 2001; 30: 470-474.

Wang EA. Bone morphogenetic proteins (BMPs): therapeutic potential in healing bony defects. *Trends Biotechnol* 1993; 11(9): 379-383.

Wang EA, Josephine VR, D'Alessandro JS, Bauduy M, Cordes P, Harada T, Israel DI, Hewick RM, Kerns KM, LaPan P, Luxenberg DP, McQuaid D, Moutsatsos IK, Nove J, Wozney JM. Recombinant human bone morphogenetic protein induces bone formation. *Proc Natl Acad Sci USA* 1990; 87: 2220-2224.

Weibrich G, Trettin R, Gnoth SH, Duschner HGH, Wagner W. Analysis of the size of the specific surface area of bone regeneration materials by gas adsorption. *Mund Kiefer Gesichtschir* 2000; 156: 1-5.

Welch RD, Jones AL, Bucholz RW, Reinert CM, Tjia JS, Pierce WA, Wozney JM, Li XJ. Effect of recombinant human bone morphogenetic protein-2 on fracture healing in a goat tibial fracture model. *J Bone Miner Res* 1998; 13: 1483-1490.

White RA, Hirose FM, Sproat RW, Lawrence RS, Nelson RJ. Histopathologic observations after short-term implantation of two porous elastomers in dogs. *Biomaterials* 1981; 2(3): 171-176.

Wozney JM. The bone morphogenetic protein family: multifunctional cellular regulations in the embryo and adult. *Eur J Oral Sci* 1998; 106(1): 160-166.

Xing Z, Kenneth S, Vecchio. Hydrothermal synthesis of hydroxyapatite rods. *J Cryst Growth* 2007; 308: 133-140.

Xu Y, Wang D, Yang L, Tang H. Hydrothermal conversion of coral into hydroxyapatite. *Mater Character* 2001; 47: 83-87.

Yasko AW, Lan JM, Fellingner EJ, Rosen V, Wozney JM, Wang EA. The healing of segmental bone defects, induced by recombinant human bone morphogenetic protein (rhBMP-2). A radiographic, histological, and biomechanical study in rats. *J Bone Joint Surg Am* 1992; 74: 659-670.

Yeom DS, Kim BI, Lee YM, Lee EJ, Yee ST, Seong CN, Seo KI, Cho HW. Relative evaluation for biocompatibility of pure titanium and titanium alloys using histological and enzymatic methods. *J Toxicol Pub Health* 2007; 23(4): 331-339.

Yokota S, Sonohara S, Yoshida M, Murai M, Shimokawa S, Fujimoto R, Fukushima S, Kokubo S, Nozaki K, Takahashi K, Uchida T, Yokohama S, Sonobe T. A new recombinant human bone morphogenetic protein-2 carrier for bone regeneration. *Int J Pharm* 2001; 223(1-2): 69-79.

Zegzula HD, Buck DC, Brekke J, Wozney JM, Hollinger JO. Bone formation with use of rhBMP-2 (recombinant human bone morphogenetic protein-2). *J Bone Joint Surg Am* 1997; 79(12): 1778-1790.

초 록

골대체재로써의 오적골에 대한 평가

(지도교수: 정 종 태)

원 상 철

제주대학교 대학원

수의학과

골대체재는 지연유합이나 유합부전 그리고 골절술과 관절고정술 시 골편의 연속성 확립이 필요한 경우 골절의 주요 결손부위를 채우는데 주로 활용되고 있다. 자가골을 대체할 수 있는 천연 골이식재의 대표적인 것이 calcium carbonate (CC)로 구성된 coral이며, 갑오징어의 오적골(Cuttlebone, CB) 또한 coral과 같은 천연 CC로 이루어져 있다. 지금까지 오적골은 몇몇 연구자들에 의해 이종골이식재로써의 가능성이 제시되어왔으나, 대부분의 연구가 해면질골에서의 실험이었으며, 체계적인 생체적합성 검사 및 편평골에서의 골형성에 관한 보고는 없었다.

본 연구에서는 오적골의 다양한 전처리 후 직경 5mm 두께 2mm의 형태로 가공하여 생체적합성 검사와 rhBMP-2의 담체로써 골진도력과 골유도력을 평가하고자 하였다.

결합조직의 두께는 2, 4주차 모두 CBHA군에서 가장 유의성 있게 얇았다 ($p < 0.05$). Radiologic Gray-level histogram의 측정에서는 4주차에서 CBHA군이 CHA군보다 유의성 있게 높게 나타났으며 ($p < 0.05$), 12주차에서는 CHA군의 변화율이 가장 적었다. 전체 12주 동안의 변화율에서는 CBHA가 가장 많은 변화를

보였다. 폐쇄율에 있어서는 4, 8, 12주차 모두 CHA군이 다른 군에 비해 유의성 있게 높게 나타났으며 ($p < 0.05$), 8주차에서는 CB1bmp 군이 CBHA군보다 유의성 있게 높게 나타났다 ($p < 0.05$).

이상의 결과들은 CBHA가 생체 내에 적용하는 골대체재로서 생체적합성이 매우 높은 것으로 나타났으며, CB1, CB1bmp, CB2보다 골유도능력에서도 그 효과가 우수한 것으로 나타났다. 따라서 CBHA는 편평골에 있어 생체적합성이 뛰어난 골대체재로 그 가치가 있는 것으로 생각되며, 수의 임상에 있어서 활용성이 매우 높을 것으로 사료된다.

중심어; 골대체제, 담체, 수산화인회석, 오적골, 탄산칼슘